Automation in Strain and Temperature Control on VHCF with an Ultrasonic Testing Facility

Lage Y.[1], Ribeiro A. M. R. [1], Montalvão D. [2], Reis L.[1] and Freitas M.[1*]

[1-] Department of Mechanical Engineering, Instituto Superior Técnico, Lisboa, Technical University of Lisbon, Av. Rovisco Pais, 1049-001 Lisbon, Portugal

* manuel.freitas@ist.utl.pt

[2-] School of Engineering and Technology, University of Hertfordshire, College Lane Campus, Hatfield,

AL10 9AB, UK

ABSTRACT

Increased safety and reliability in mechanical components became a subject of prime importance over the past recent years. Therefore, a proper understanding of damage and fracture mechanics in materials and components designed to withstand Very High Cycle Fatigue (VHCF) loadings is extremely important nowadays. However, conventional machines used for fatigue testing are very time-consuming and costly in order to perform VHCF tests. Ultrasonic machines have been introduced as a way to increase the number of cycles in fatigue testing up to $1E^8$ to $1E^{10}$ cycles within a considerably reduced amount of time. Nevertheless, the accurate measurement of the parameters that influence fatigue life at ultrasonic frequencies (e.g., stress, displacement, strain-rate, temperature and frequency) is still a matter of concern and on-going development. Due to the high frequencies involved in VHCF testing, a huge amount of heat is generated over the specimen, which greatly affects the variables determining the fatigue behavior.

This paper describes the design and instrumentation of an ultrasonic fatigue testing machine that operates at 20 kHz working frequency. Among other features, it incorporates automated strain and temperature control. In order to run automated tests, a closed loop monitoring and control system was developed based on the measured temperature and displacement amplitudes. Temperature readings are made with a pyrometer and thermography camera and displacement is monitored at the free end of the specimen with a high resolution laser. The machine's power output is continuously adjusted from the displacement readings, so that the stress variations within the specimen are as flat as possible. When temperature increases above a certain set value, a cooling function is triggered and the test is interrupted until the specimen is cooled down. Data is acquired, managed and processed with a data acquisition device working at 400 kHz sampling frequency.

The advantages and limitations of metal fatigue testing at very high frequencies are discussed in this paper, with special emphasis on the strain and temperature control issues. Comparison of tests carried out with and without both displacement and temperature control are made on two metallic alloys, copper 99% and carbon steel, with the determination of S-N curves.

KEYWORDS

Very High Cycle Fatigue (VHCF), ultrasonic fatigue testing, amplitude control, temperature control, experimental tests.

1 Introduction

The increasing need for faster measurements in fatigue combined with improvements in piezoelectric technology, made of ultrasonic testing an attractive technique to establish S-N curves in Very High Cycle Fatigue (VHCF). The piezoelectric technique was started by Hopkinson in the beginning of the 20th century. Fifty years later, Mason presented the first ultrasonic fatigue testing machine working at 20 kHz. These were the early days of VHCF and other machines operating at higher frequencies followed, but the difficulties to correlate results constituted a hindrance that slowed down the development of this technique.

Recent advances on sensor technology, new computational methods and faster control systems, made it possible to tackle some of the problems related to VHCF. However, the accuracy on the determination of applied stresses and issues related to temperature control of the specimens when tested at very high frequencies, still constitute a challenge.

Latest developments in the ultrasonic technique are presented by Bathias *et al.* [1-5]. An extensive review of the fundamentals on VHCF fatigue using ultrasonic methods, including considerations on the machine development, its performance and applications, can be found in these works. It has been observed that specimens are subjected to very large temperature increases in ultrasonic fatigue testing, as a result of internal friction. Temperature has been pointed as the most significant variable affecting results in VHCF [6]. As an attempt to gain control over temperature, the specimen can be cooled down with cooling fluids. Nevertheless, some fluids may lead to changes on the mechanical properties of the specimen's surface and, thus, condition results.

In the more recent works presented by Stefanie Stanzl-Tschegg *et al.* [7-8], the principles and testing procedures of very high cycle fatigue tests are overviewed. Findings in the areas of crack formation, non-propagation of small cracks, long crack propagation and thresholds, effects due to frequency, superimposed and variable amplitude loading, are reported and discussed as well.

Many other publications can be found using the concept of ultrasonic waves in fatigue. In Mayer [9, 10], cyclic torsion and cyclic tensile–compression fatigue experiments are performed on aluminum alloy 2024-T351. These tests are conducted both in the high and very high cycle fatigue regimens with either constant or variable amplitudes. Müller and Sander [11] quantify the effect of the variable amplitude loadings and monitor crack growth. Sohar et al. [12] describe investigations on surface cracks nucleation and propagation on AISI D2 cold work tool steel in the gigacycle regimen. Zimmermann et al. [13] study the effects of particle strengthening and high temperature on the VHCF behavior of hardened nickel-base alloy Nimonic 80A. There are many other authors that have published in the area of ultrasonic fatigue as well, for instance [14-17].

The VHCF regimen is now an established technology in what concerns the layout of ultrasonic fatigue machines. Nevertheless, the accurate measurement of the variables that influence fatigue life (stress, displacement, temperature, etc.) at ultrasonic frequencies is still a matter of concern and continuous development by the scientific community.

2 Ultrasonic Fatigue Concept

An ultrasonic fatigue test differs from the conventional fatigue in the *nature* of vibration. An ultrasonic test seeks to reproduce free vibration with the specimen vibrating at its own fundamental frequency. In conventional testing the working frequency is set away from the fundamental frequencies (often below the fundamental frequency) and the specimen is subjected to forced vibration. In order to perform ultrasonic tests, it is necessary to design a specimen with a fundamental frequency that is tuned to match the machine's working frequency.

Ultrasonic fatigue machine is based on the concept of free vibration. Elastic wave theory can be used to explain this concept, in particular, the theory of longitudinal waves which propagate through a solid material. Longitudinal waves are propagated throughout the specimen and the displacement of its particles is parallel to the direction of the wave propagation. The speed of these waves is dependent on the material's properties and path geometry.

2.1 Longitudinal elastic waves - Formulation for the specimen's design

The specimen is designed in such a way that, under longitudinal resonance [1], its response satisfies the differential equation of motion (1):

$$\frac{\partial^2 u(x,t)}{\partial x^2} + P(x)\frac{\partial u(x,t)}{\partial x} = \frac{1}{C^2}\frac{\partial^2 u(x,t)}{\partial t^2} \tag{1}$$

where $C = \sqrt{\frac{E_d}{\rho}}$ is the wave propagation velocity, $P(x) = \frac{S'(x)}{S(x)}$ is the cross sectional area ratio, E_d is the dynamic Young's modulus and ρ is the mass density.

The solution of the differential equation of motion takes the form:

$$u(x,t) = U(x)\sin(\omega t) \tag{2}$$

where ω is the resonant frequency in rad/s. The amplitude of vibration $U(x)$ along the specimen can be determined at each point from:

$$U''(x) + P(x)U'(x) = -\frac{\omega^2}{C^2}U(x) \tag{3}$$

The specimen's geometry can be described by being composed by two well determined parts (see Fig. 1): a cylindrical one and another with variable cross-section obtained from the revolution of a hyperbolic cosine about the middle axis. These are expressed by the following functions:

$$\begin{aligned} y(x) &= R_2, \quad L_2 < |x| < L \\ y(x) &= R_1 \cosh(\alpha x), \quad |x| \le L_2 \end{aligned} \tag{4}$$

where: $L = L_1 + L_2$ and $\alpha = \frac{1}{L_2} arc\cosh\left(\frac{R_2}{R_1}\right)$

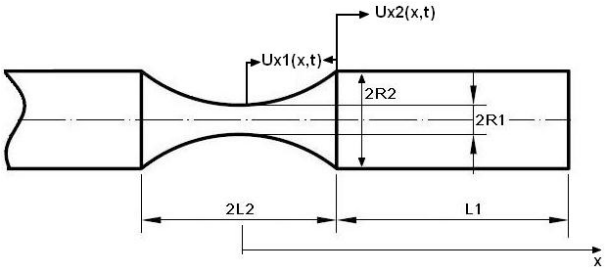

Fig. 1 Standard specimen test geometry.

Once the appropriate boundary conditions and resonant frequency are determined, the solutions for the longitudinal displacements along the specimen are obtained:

$$u_1(x,t) = A_0 \frac{\cos(kL_1)\cosh(\alpha L_2)}{\sinh(\beta L_2)} \frac{\sinh(\beta x)}{\cosh(\alpha x)} \sin(\omega t), x < L_2 \tag{5}$$

$$u_2(x,t) = A_0 \cos(k\left(L-x\right)) \sin(\omega t), L_2 < x \leq L \tag{6}$$

with:

$$k = \sqrt{\frac{\omega^2}{C^2}} \tag{7}$$

$$\beta = \sqrt{\alpha^2 - k^2} \tag{8}$$

where A_0 is the displacement amplitude at the free-end of the specimen.

Eqs. (5) and (6) are used to obtain both stress σ and strain ε at any location x:

$$\varepsilon(x,t) = \frac{\partial u(x,t)}{\partial x} \tag{9}$$

$$\sigma(x,t) = E_d\, \varepsilon(x,t) \tag{10}$$

This analytical solution is used to determine the specimen's dimensions, so that the first longitudinal vibration mode is tuned with the exciting frequency. Note that, in deducting the exact equations, a hyperbolic cosine was used to define the variable cross-section, but, in practice, a circular profile is used. This is due to the manufacturing advantages related to the milling process of the specimens. Nevertheless, it is possible to demonstrate that this is a good approximation, which error does not exceed 1.8% [1].

Fig. 2 shows the evolution of displacement and stress along the typical specimen geometry, when calculated by the analytical Eqs. (5), (6) and (10).

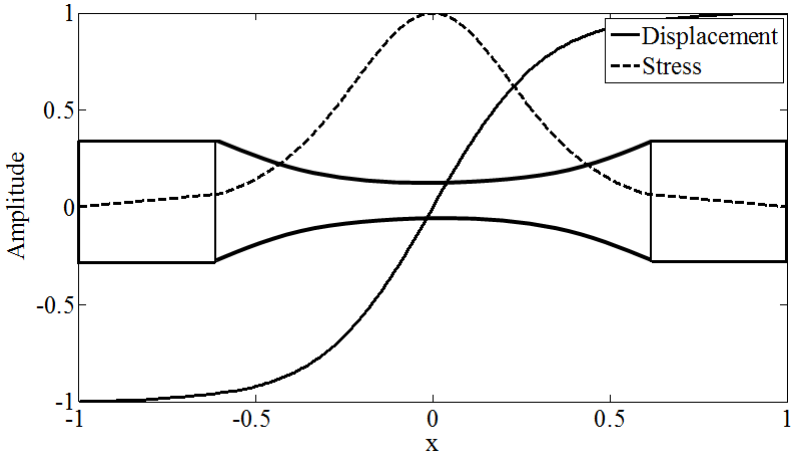

Fig. 2 Distribution of displacement and stress on the specimen.

3 Ultrasonic Fatigue testing machine

In an ultrasonic fatigue testing machine, the displacement imposed by the piezoelectric actuator must be transmitted along a series of resonant elements connected together. The specimen is at the end of this series of elements and the displacement is measured at its free end. The stress level is determined as a function of the displacement. Due to the very specific geometrical properties of the elements, the amplitude of vibration changes from the actuator to the specimen's free end, which translates into different levels of axial stresses being developed along the elements.

When designing an ultrasonic fatigue testing machine, the primary concern is that the whole system's longitudinal fundamental frequency is the same as the working frequency of the exciter. Next, comes monitoring and control. The ultrasonic fatigue testing machine must be able to monitor and control parameters like temperature, stress level, frequency and power output.

The first version of the ultrasonic fatigue testing machine being discussed in this paper is presented in [18, 19].

3.1 General Machine Setup

The setup of the ultrasonic fatigue testing machine presented herewith is identical to some other existing ones. Differences emerge regarding the type of sensors used and on the monitoring and control features. The machine integrates four main systems, which are illustrated in Fig. 3:

- resonant system;
- cooling system;
- measurement system;
- data acquisition, processing and control system.

These four systems work together to carry out fatigue tests within the ranges initially set of temperature, stress level, etc.

The *resonant system* incorporates an ultrasonic piezoelectric exciter that is used to excite the system to its fundamental axial frequency. It works in the 19.5-20.5 kHz

range. A power setting may be changed, so that the displacement at the free-end of the specimen can be adjusted.

The *cooling system* is composed by two fans, helping to cool the resonant system and specimen during the different test phases.

The *measurement system* is composed by several sensors. A high resolution laser Doppler vibrometer and an optional strain gauge are used for acquiring, respectively, the displacement at the free end of the specimen and the strain at its center. Two analog input channels are used to acquire these signals with a sampling frequency up to 200 kHz, or 400 kHz if only one channel is used. A pyrometer is used for monitoring the temperature at the narrow center section of the specimen and a thermography camera to plot temperature distribution and gradients along the specimen.

The *data acquisition, processing and control system* deals with all the monitoring and control inputs and outputs. It controls the resonant system with a closed loop feedback system that continuously monitors the stress level and working frequency. A computer program was developed under LabVIEW®, which also serves as interface with the user.

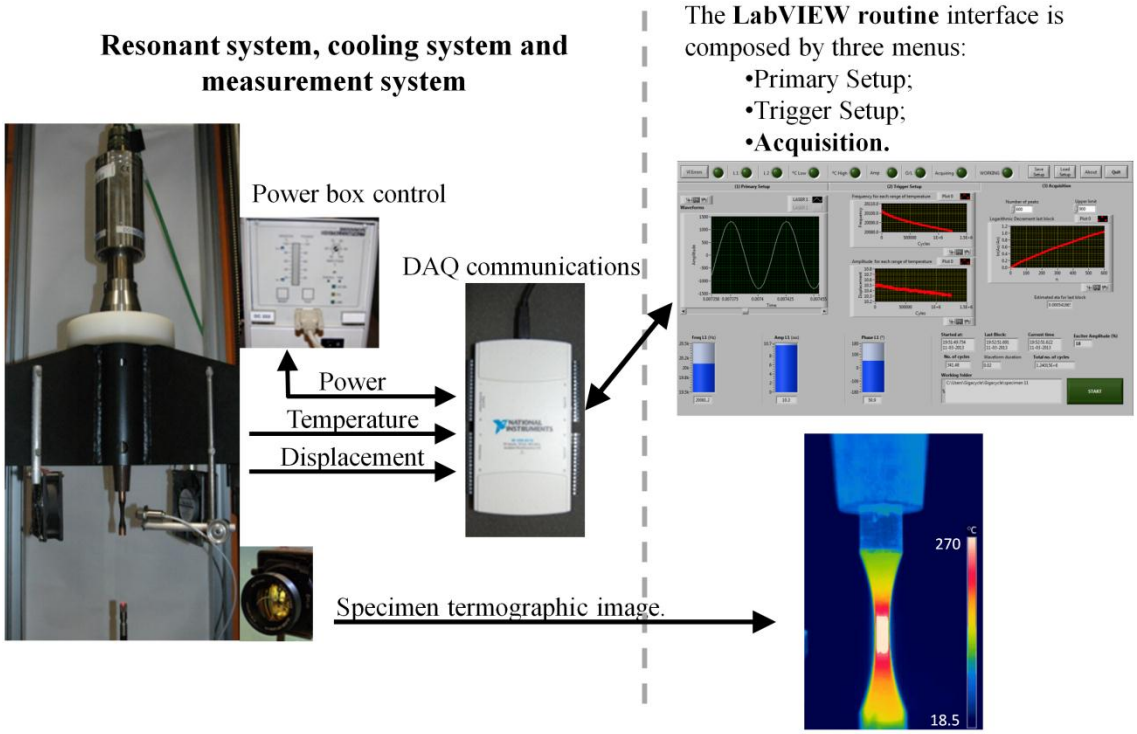

Fig.3 Main parts of the ultrasonic fatigue machine setup.

3.2 Resonant system

The resonant system is composed by a piezoelectric actuator, booster, horn and specimen. These are assembled together in a sequence by screw connections. These four parts form the resonant system of the testing machine and are shown in Fig. 4(a). The mechanical vibration generated by the piezoelectric exciter is meant to reproduce a pure sine wave with a frequency of 20 kHz approximately. This wave is transmitted from element to element down to the end of the specimen. The principle of operation of the

vibration system is based on free vibration resulting in a minimum of contact force between the elements in the system.

Each element in the resonant system is manufactured to have the same axial fundamental frequency and vibrate in phase opposition, as depicted in Fig. 4(b). Thus, tight tolerances have to be used and manufacturing needs to be very precise. If a single element in the system does not have the same axial fundamental frequency – within a tolerance of 2.5% – the actuator is not capable to operate and the system is shut down.

To verify that the system is working as intended, the dynamic response can be measured at the bottom of the specimen. The time signal must be as close as possible to a pure sine wave, which is represented by a single peak in the Fourier Spectrum. Fig. 5 shows that only residual spectral components exist, with peak amplitudes less than 0.1% of the fundamental peak frequency at 20 kHz. To evaluate the quality of the time signal, a total harmonic distortion (THD) of the fundamental harmonic was computed using a standard LabVIEW® routine, resulting in a 1.594% harmonic distortion. The routine was set up to include up to the 10^{th} harmonic at 200 kHz.

Power delivered to the piezoelectric actuator is controlled by a signal generator. A closed-loop feedback algorithm is used to keep the displacement amplitude constant by adjusting the power setting.

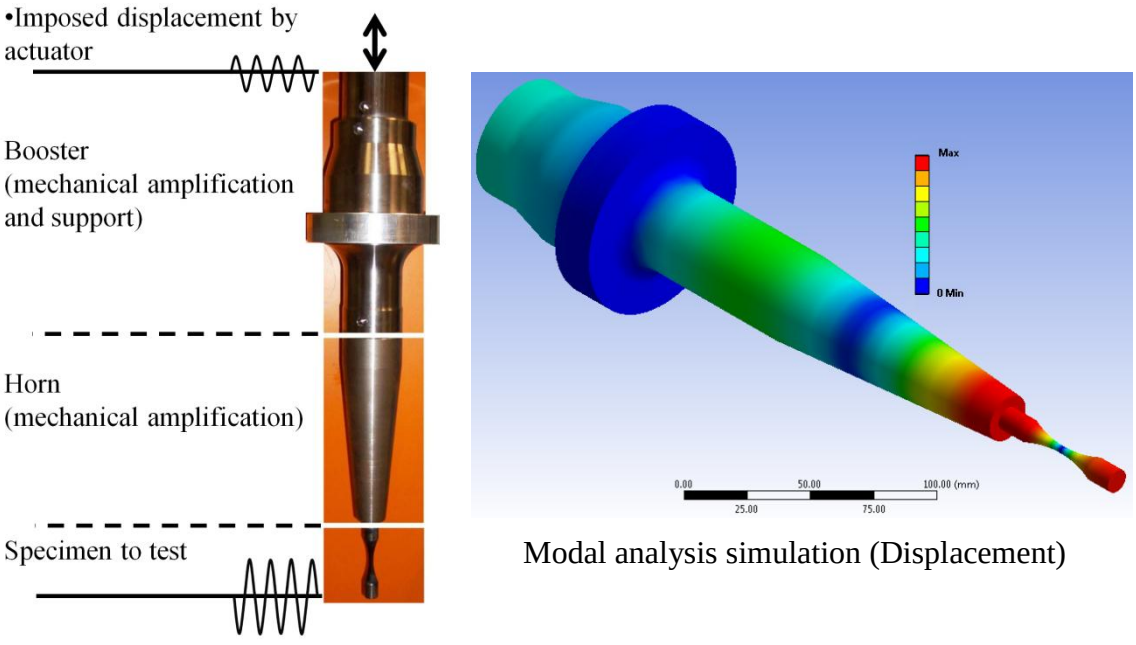

Modal analysis simulation (Displacement)

(a) (b)

Fig.4 (a) resonant system components; (b) modal analysis simulation for the first axial mode at 20 kHz.

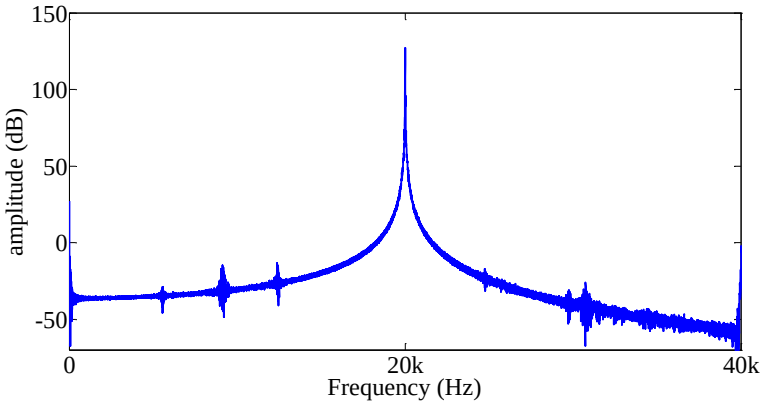

Fig.5 Fourier spectrum of the signal measured at the bottom of the copper specimen, fundamental frequency at 20013 Hz.

3.3 Cooling System

Vibrational energy delivered by the piezoelectric actuator is dissipated along the resonant elements by damping phenomena. Significant heat is generated and cooler fans are used to speed up the process of bringing temperature back to normal. The configuration of the cooling system is shown in Fig. 6, with balloon number 5 pointing to one of the two existing fans.

3.4 Measurement System

The measurement system integrates the sensors needed to measure the dynamic parameters of the specimen. Their locations are illustrated in Fig. 6 and include:

- high resolution laser vibrometer (1), to measure the dynamic response at the bottom of the specimen;
- strain gauge (2), to measure the dynamic strain at the middle section of the specimen;
- pyrometer (3), to monitor the value of temperature at the middle section of the specimen;
- thermography camera (4), to map the distribution of the temperature on the surface of the specimen.

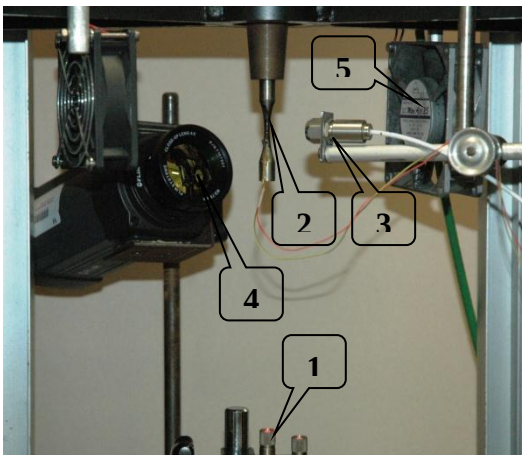

Fig. 6 Configuration of the measurement system

The stress at the center of the specimen (nodal point) can be determined from the laser measurement at its end (Eq. (11)). If the the strain gauge is used, the stress level can be determined directly from Eq. (12). However, the use of a strain gauge has limitations, since its own fatigue life is quite short when compared to the whole test duration.

$$\sigma_{laser} = E_d \left| \frac{\partial u}{\partial x} \right|_{x=0} \tag{11}$$

$$\sigma_{strain\ gauge} = E_d\, \varepsilon \tag{12}$$

3.5 Data acquisition, processing and control system

An in-house custom made package was developed under LabVIEW® from National Instruments (NI) for online monitoring and control of the VHCF machine. Communication between the peripherals and the software is done using a multifunction data acquisition (DAQ) device from NI (NI USB-6216). The NI USB-6216 is a multiplexed 16 bit DAQ with a maximum analog input sampling frequency of 400kS/s. It can measure up to 16 analog signals at a time and has 32 digital TTL inputs and outputs.

This computer software is the main interface with the user. It allows setting up the initial testing frequency and initial power delivered to the piezoelectric actuator, based on a pre-determined value for the axial stress. It also indicates and logs the specimen's temperature, displacement, frequency, power delivered to the piezoelectric exciter and number of cycles until fracture. Furthermore, it includes an algorithm to estimate and monitor the damping ratio evolution during the whole test. When the fatigue test is finished, a summary with the monitoring history is shown on the computer screen and stored into a spreadsheet file.

This package includes three main displays:

(1) Primary Setup menu (Fig. 7) – The measurement channels and acquisition settings are set up in this menu, namely the sampling frequency and the time duration of an acquisition block. These settings are related to the nature of the continuous acquisition process in LabVIEW. One run is composed by a finite number of time signal blocks. Each block is then "averaged" to extract amplitude and frequency. Long blocks may produce inaccurate results due to the rapid change in both temperature and frequency, whereas short blocks may produce instability due to the need of faster processing capabilities. The Primary Setup also offers the possibility of setting the displacement value at the tip of the specimen. During measurement, a closed-loop feedback system adjusts the exciter's power so that the average displacement per block is constant;

(2) Trigger Setup menu (Fig. 8) – The trigger setup offers the possibility to test the performance of the configuration set on the primary setup. This interface is also used to determine delays in the exciter that are very hard to predict otherwise. Once the primary settings are set and the triggers have been determined, there is no need to run the trigger setup again;

(3) Acquisition display (Fig. 9) – The acquisition display shows the current time signal block and the history for a single run. It plots the frequency evolution per block,

the average displacement per block and the logarithmic decrement in the last block. The last block is a transient response time signal of the resonant system at free vibration, giving information on the damping factor.

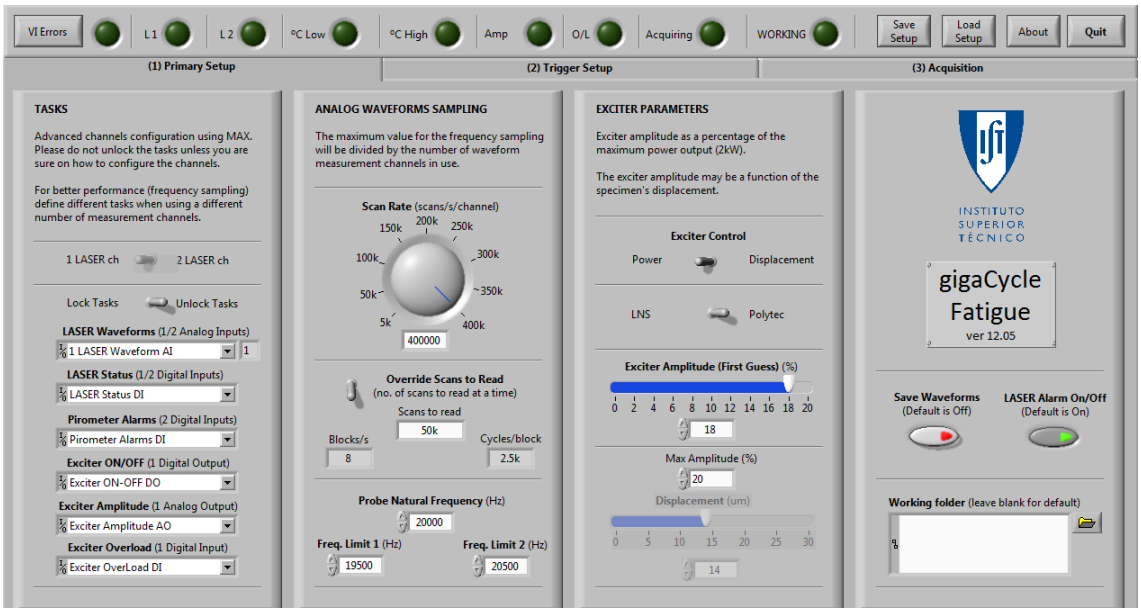

Fig. 7 LabVIEW software's primary setup.

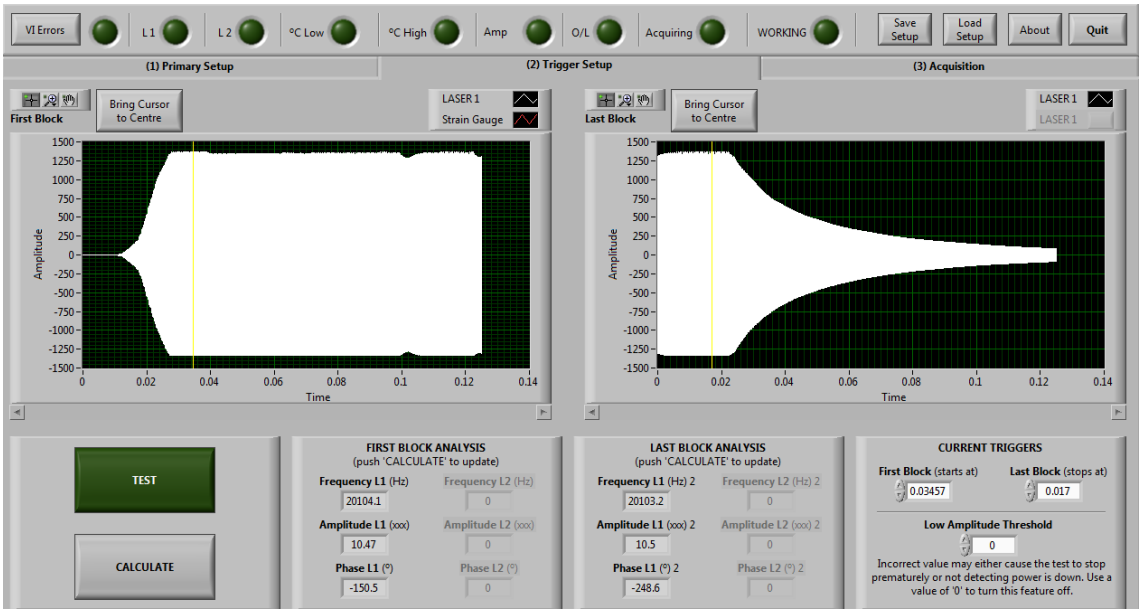

Fig. 8 LabVIEW software's trigger setup.

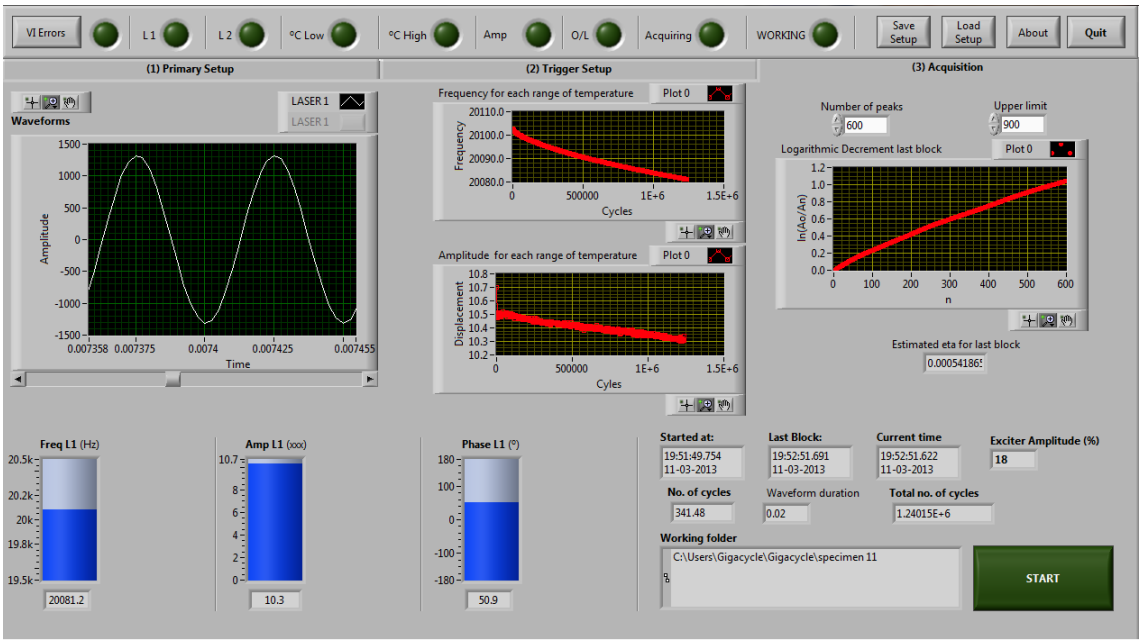

Fig. 9 LabVIEW's software's acquisition display.

3.5.1 Hysteretic damping estimation method

One feature that the discussed machine offers is to provide an estimation of the energy dissipated by the material during the test. For a hysterically damped single-degree-of-freedom system harmonically excited and at steady-state, the energy ΔE dissipated per cycle of oscillation may be defined as [20]:

$$\Delta E = \int_0^{2\pi/\omega} f(u)\,du = \pi U^2 d \quad \text{with} \quad d = \eta k \tag{13}$$

where $f(x)$ represents the dynamic force, U is the displacement peak amplitude per cycle, d the hysteretic damping coefficient, k the stiffness and η the hysteretic damping loss factor. When plotted on a force *vs* displacement graph, the energy dissipated per cycle of oscillation takes the form of an ellipse area.

Eq. (13) is used on steady state conditions, when the applied force is known. When the system is subjected to free vibration, the hysteretic damping loss factor may be estimated by Eq. (14) instead [21]:

$$\delta = \frac{1}{n}\ln\left(\frac{U_i}{U_{i+n}}\right) = 2\pi\frac{\eta}{1+\sqrt{1+\eta^2}} \quad \text{thus} \quad \eta = \frac{4\pi\delta}{4\pi^2-\delta^2} \tag{14}$$

where δ is the logarithmic decrement and n is the number of cycles between peak amplitudes U_i and U_{i+n}.

In the LabVIEW routine Eq. (14) is used as follows:

$$n_j\delta_j = \ln\left(\frac{U_i}{U_{i+n_j}}\right) \text{ with } j = 1,\ldots,n \tag{15}$$

For example, if a signal with exponential decay envelope is considered as in Fig. 10(a), Eq. (15) yields the results shown in Fig 10(b), in which the slope is the logarithmic decrement.

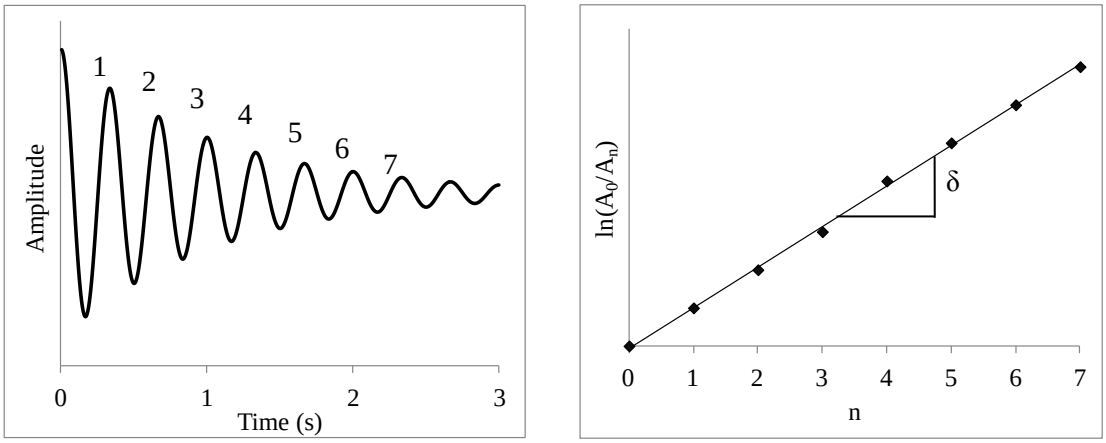

(a) (b)

Fig. 10 Algorithm implemented in LabVIEW to determine the logarithmic decrement and the hysteretic damping loss factor.

Although the hysteretic damping loss factor can be estimated, the discussion on its performance and correlation with fatigue is left aside of this work for future discussion. However, as an example of the possible outcomes, Fig. 11 shows the hysteretic damping factor (η) for ultrasonic fatigue test carried out with a temperature in the [40-60] º C range and a middle section stress of 372 MPa (R = -1) for low carbon steel.

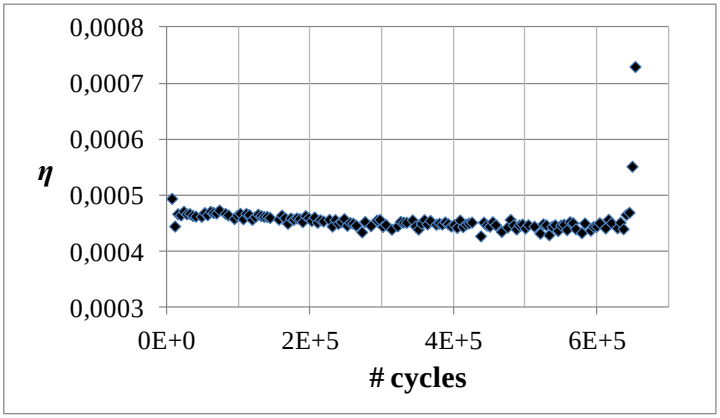

Fig. 11 Typical hysteretic damping behavior to ultrasonic test for low carbon steel (not discussed in this paper).

3.5.2 Parameters control

When performing an ultrasonic fatigue test without any type of feedback control, the piezoelectric system delivers a constant power output continuously. Temperatures may increase to very high levels and, in some materials, values greater than 300 ºC have been registered. The increase in temperature has a strong effect on the displacement amplitude and, thus, on the stress amplitudes being generated. In order to keep displacement and stress as steady as possible, two control algorithms based on the measured test parameters were implemented. These algorithms are integrated in the LabVIEW package and are based on *temperature control* and *amplitude control*. Both controls can be operating together or independently. The current control functions are updated versions since the first attempt described in [22, 23].

In *basic test setup* the power provided to the piezoelectric actuator is set and there is no feedback-loop control. The fatigue test starts and runs continuously, without interruption, at 20k cycles/second. The signals from the laser and pyrometer are acquired and stored in order to monitor the specimen. The displacement amplitude per measurement period of time (block) is the average of the values measured at steady state. Because the test runs continuously, the temperature will eventually rise to a value outside an acceptable range.

In *temperature control* the fatigue test runs as long as temperature is kept within an preset interval ΔT. Temperature is continuously monitored while the test is in progress, while at the same time amplitude, frequency and power are measured and stored. When temperature reaches the upper limit, the test is interrupted. The specimen cools down until temperature reaches the lower preset value and is restarted. This process is illustrated in the "saw tooth" plot Fig. 12. Temperature control contributes to the stability of the vibration amplitude during test but it does not eliminate it completely.

With *amplitude control* activated, the displacement is monitored at the free end of the specimen during each period of time (block). The piezoelectric actuator's power is continuously readjusted between blocks to keep the vibration amplitude at a constant pre-established value.

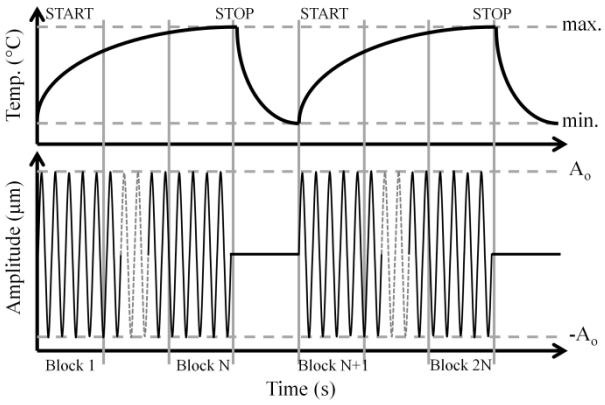

Figure 12. Illustration of record signal with amplitude/temperature control.

4 Experimental procedure in VHCF tests

4.1 Testing materials

Two different types of materials, copper (99%) and carbon steel like the one used in railroads, were tested.

The material properties are described in Table 1 where E_d, ρ, YS and UTS represent, respectively, the dynamic Young's modulus, the material's density, the yield stress and the ultimate tensile strength.

Table 1. Material properties.

	E_d [GPa]	ρ [kg/m^3]	YS [MPa]	UTS [MPa]
Copper	106	9019	272	285
Steel	196	7850	455	800

The specimen dimensions for each of the materials tested are presented in figures 13 and 14.

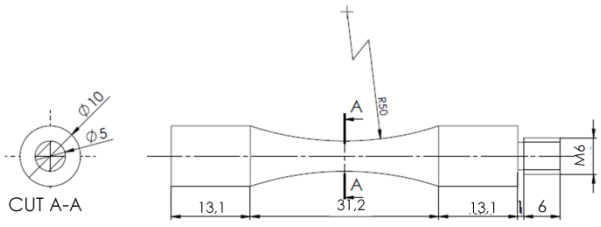

Figure 13. Dimensions of the copper specimen.

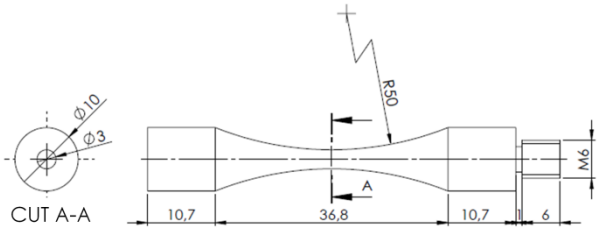

Figure 14. Dimensions of the Carbon steel specimen.

4.2 Parameters configuration

The specimens' dimensions shown in section 4.1 were determined according to the formulation described in section 2.1, so that, after manufacturing, the longitudinal fundamental frequency matches 20 kHz, approximately (the actuator's power box can only operate in the 19.5 kHz to 20.5 kHz frequency range).

In the present experimental examples, the sampling frequency was set at 400 kHz and the duration for an acquisition block was set at 0.125 s. Hence, the feedback loop update occurred every 2500 cycles.

After testing several specimens of each material, either with amplitude control, temperature control or both, S-N curves were plotted. Table 2 presents a summary of the amplitude and temperature test specifications for each of the specimens considered.

Table 2. Amplitude and temperature test specifications.

Amplitude and Temperature test specification		
Copper	With and without Amp. control	All with Temp. control 45-50 ºC
Carbon steel	All without Amp. control	With Temp. control 40-60 ºC and without.

5 Results and discussion

VHCF tests were performed at 20 kHz for different stress amplitudes under fully reversed cyclic loading (R= -1). Also, as mentioned before, different types of control (amplitude control, temperature control and both) were considered. Because the objectives of the present work are related to the study of VHCF only, S-N curves will be plotted for $1E^6$ up to $1E^9$ cycles only.

5.1. S-N Curves

S-N results obtained for tests on copper are presented in Fig. 15. It is clear that the S-N data shows a typical behavior for this type of material. Also, stress amplitudes are within the expected levels.

When ultrasonic tests were performed on carbon steel without temperature control, enormous amounts of heat were dissipated at the center of the specimen. With uninterrupted testing conditions, the specimen reached temperatures up to 270 ºC within just a few seconds. Fig. 16 shows both the S-N results for carbon steel with temperature control (in the range of [40 - 60] ºC) and without temperature control. Results from the literature are also shown [24], for comparison.

With temperature control, tests were performed in the [45 - 50]ºC range for Copper and in the [40 - 60]ºC for Steel. These ranges were established to be as narrow and low as possible, so that effects due to temperature in the fatigue process can be neglected.

With respect to the use of amplitude control in Copper, it was concluded that it did not change the appearance of the S-N plot. This can be explained because temperature control restricts the variation of other control parameters (that depend on temperature themselves, like the amplitude of vibration). Since the temperature control was set at a very narrow range, the use of amplitude control together with temperature control became redundant.

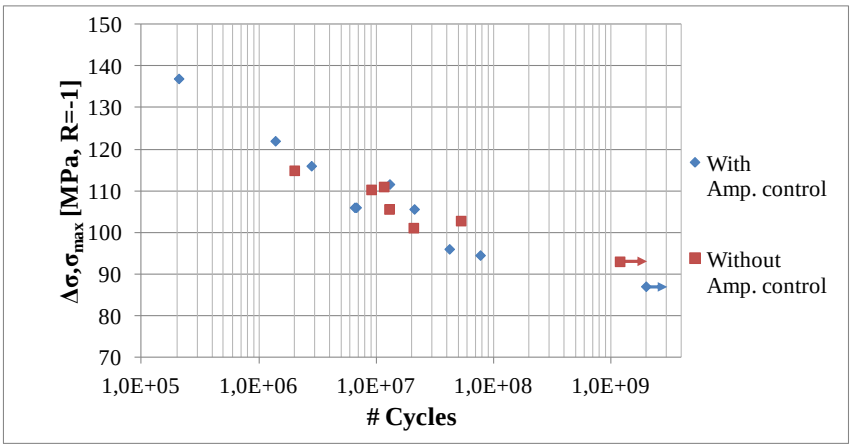

Figure 15. Copper S-N curve.

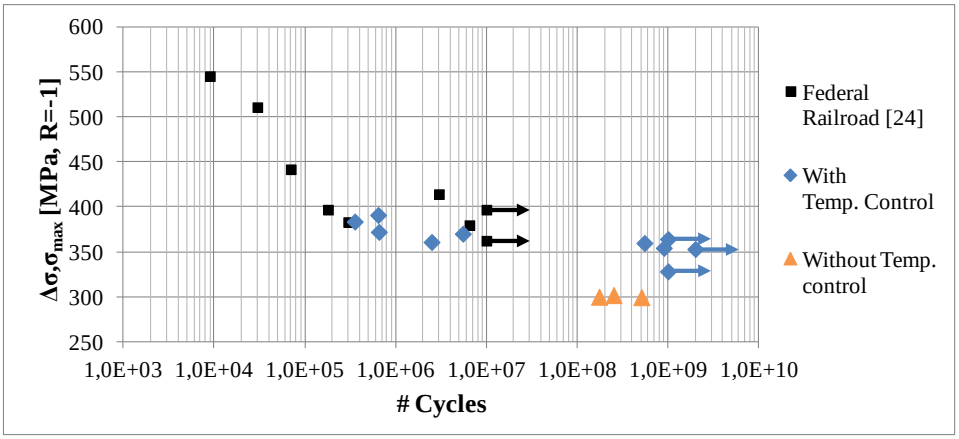

Figure 16. Carbon steel S-N curve.

From the analysis of Fig. 16, it is possible to verify that the experimental results obtained near to $1E^6$ cycles in the [40 - 60]ºC temperature range, are similar to those presented in the literature (Federal Railroad [24]). Furthermore, the material performance up to $1E^9$ cycles with temperature control is consistent as well.

Without temperature control, fracture occurred for lower levels of stress: less than 55 MPa (or 15%) than when temperature control was used. In this case, ultrasonic fatigue tests were performed at 270ºC and over.

5.3. Fractography

In VHCF, fracture may occur due to either internal or external cracks [1]. All fractured specimens were observed in an optical microscope. Sample photographs are shown in Figs. 17 and 18 for copper and steel, respectively.

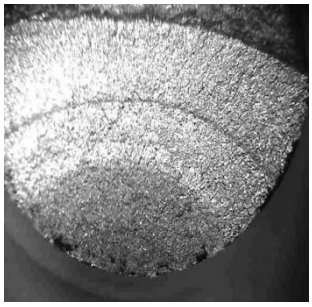

Figure 17. Copper fracture surface (94.5 MPa; $7.7E^7$ cycles).

Fig. 17 shows that, for copper, the crack initiates and grows from the surface of the specimen. All the three stages of fatigue are clear: crack initiation, propagation and fracture. It is still possible to observe typical “beach marks”.

In contrast, Fig. 18 shows that, for carbon steel, the crack initiated in the interior of the specimen. It is clearly observed a “fish-eye” pattern, very characteristic of VHCF failures in steel. The fish-eye fracture is characterized by a “Fine Granular Area” (FGA) in the vicinity (and around) of an inclusion. A Scanning Electron Microscope was used to examine the FGA.

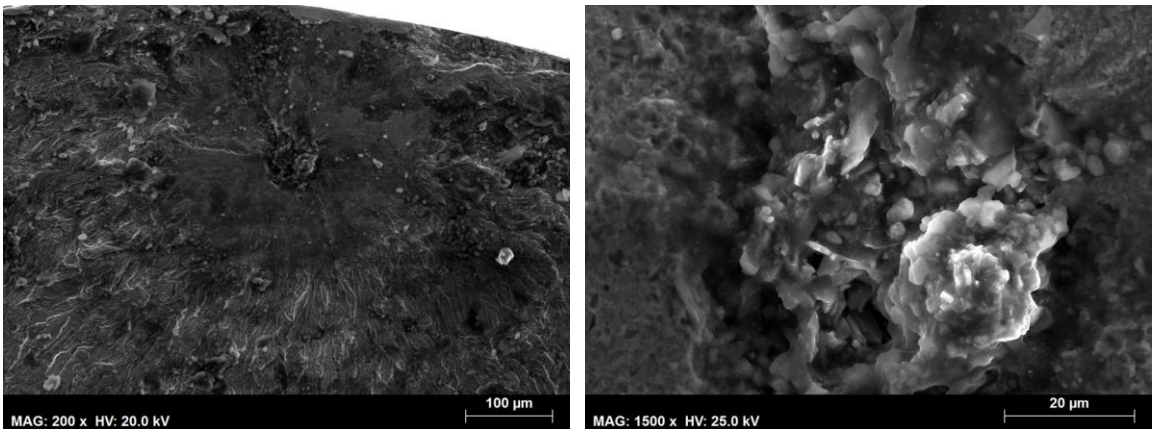

Figure 18. Carbon Steel "Fish-eye" fracture surface (360 MPa; 5.5E^8 cycles).

6 Conclusions

The operation and testing of an ultrasonic fatigue testing machine was presented and discussed.

The exciter's horn and specimen were designed so that their axial fundamental frequencies would be tuned with the piezoelectric actuator working frequency (20 kHz).

The instrumentation of the machine allowed monitoring the specimen's temperature and displacement amplitude in a closed loop control fashion. Data acquisition, monitoring and control were done with a custom made package developed under the LabVIEW® platform.

A method to estimate the hysteretic damping factor evolution during fatigue tests is presented as well as an indirect way to measure damage in the specimen.

A set of experimental tests using the presented ultrasonic fatigue testing machine were carried out, using two types of controls:

- temperature control, with the temperature measured at the area of maximum stress of the specimen (node at the middle), ensuring that the specimen does not exceed the pre-defined temperature limits;
- amplitude control, with the displacement level measured at the bottom of the specimen, ensuring that the stress level is kept constant during the whole test.

S-N curves were obtained for copper and carbon steel, showing typical behaviors for these materials that are in good agreement with the available literature.

References

[1] Bathias C., Paris P. C., Gigacycle fatigue in mechanical practice. New York: Marcel Dekker, 2005.

[2] Bathias C, Piezoelectric fatigue testing machines and devices, International Journal of Fatigue 28, 2006, 1438–1445.

[3] I. Marines, X. Bin, C. Bathias, An understanding of very high cycle fatigue of metals, International Journal of Fatigue 25 (2003) 1101–1107.

[4] C. Bathias, L. Drouillac, P. Le François, How and why the fatigue S–N curve does not approach a horizontal asymptote, International Journal of Fatigue 23, 2001, S143–S151.

[5] Bathias C, Paris P. C., Gigacycle fatigue of metallic aircraft components, International Journal of Fatigue 32, 2010, 894–897.

[6] Claude Bathias, Influence of the metallurgical instability on the gigacycle fatigue regime, International Journal of Fatigue 32. 2010. 535–540.

[7] Stanzl-Tschegg, S., Very high cycle fatigue measuring techniques, International Journal of Fatigue (2012), doi: http://dx.doi.org/10.1016/j.ijfatigue.2012.11.016.

[8] S. Stanzl-Tschegg, B. Schönbauer, Near-threshold fatigue crack propagation and internal cracks in steel, Procedia Engineering 2, 2009, 1547-1555.

[9] Mayer H., Ultrasonic torsion and tension–compression fatigue testing: Measuring principles and investigations on 2024-T351 aluminium alloy. International Journal of Fatigue, 2006, 28, 1446 – 1445.

[10] H. Mayer et al., Constant and variable amplitude ultrasonic fatigue of 2024-T351 aluminium alloy at different load ratios, Ultrasonics (2013), http://dx.doi.org/10.1016/j.ultras.2013.02.012.

[11] T. Müller, M. Sander, On the use of ultrasonic fatigue testing technique – Variable amplitude loadings and crack growth monitoring, Ultrasonics (2013), http://dx.doi.org/10.1016/j.ultras.2013.03.005.

[12] Christian R. Sohar, Agnieszka Betzwar-Kotas, Christian Gierl, Brigitte Weiss, Herbert Danninger, Fractographic evaluation of gigacycle fatigue crack nucleation and propagation of a high Cr alloyed cold work tool steel, International Journal of Fatigue 30, 2008, 2191–2199.

[13] M. Zimmermann, C. Stöcker, H.-J. Christ, On the effects of particle strengthening and temperature on the VHCF behaviour at high frequency, International Journal of Fatigue 33, 2011, 42–48.

[14] Zhi Yong Huang, Danièle Wagner, Claude Bathias, Jean Louis Chaboche, Cumulative fatigue damage in low cycle fatigue and gigacycle fatigue for low carbon–manganese steel, International Journal of Fatigue 33, 2011, 115–121.

[15] Y. Yu, J.L. Gu, F.L. Shou, L. Xua, B.Z. Bai, Y.B. Liu, Competition mechanism between microstructure type and inclusion level in determining VHCF behavior of bainite/martensite dual phase steels, International Journal of Fatigue 33, 2011, 500–506.

[16] C. Müller-Bollenhagen, M. Zimmermann, H.-J. Christ, Very high cycle fatigue behaviour of austenitic stainless steel and the effect of strain-induced martensite, International Journal of Fatigue 32, 2010, 936–942.

[17] Y. Furuya, Specimen size effects on gigacycle fatigue properties of high-strength steel under ultrasonic fatigue testing, Scripta Materialia 58, 2008, 1014–1017.

[18] Freitas M, Reis L, Anes V, Montalvão D, Ribeiro AM and Fonte M. Design and assembly of an ultrasonic fatigue testing machine, Anales de Mecânica de la Fractura, 29, Vol. 1, 335 – 340.

[19] Anes V, Montalvão D, Ribeiro AM, Freitas M and Fonte M. Design and instrumentation of an ultrasonic fatigue testing machine. Proceedings of the 5th

International Conference on Very High Cycle Fatigue, Berlin, Germany, 2011, 421 – 426.

[20] N. M. M. Maia and J. M. M. e Silva, Theoretical and experimental modal analysis, Research Studies Press LTD., 1997.

[21] Ribeiro, A.M.R., Maia, N.M.M., Silva, J.M.M., Reis, L., Freitas, M., Free vibration response using the constant hysteretic damping model, Scientific Bulletin of the "Politehnica" University of Timisoara, Romania, Transactions on Mechanics, Vol. 50(64), Actas da XIth International Conference on Vibration Engineering, Timisoara, Romania, September, 2005, 65-70.

[22] Lage, Y., Freitas, M., Montalvao, D., Ribeiro, A. M. R and Reis, L., Ultrasonic Fatigue Analysis on Steel Specimen with Temperature Control: Evaluation of Variable Temperature Effect, XIII Portuguese Conference on Fracture, Coimbra, Portugal, 2012.

[23] Lage, Y., Freitas, M., Reis, L., Ribeiro, A. M. R. and Montalvao, D., Instumentation of Ultrasonic High-Frequency Machine to Estimate Applied Stress in Middle Section of Specimen, 15th International Conference on Experimental Mechanics, Porto, Portugal, 2012.

[24] Fatigue Behavior of AAR Class A of Transportation Railroad Wheel Steel at Ambient and Elevated Temperatures, Federal Railroad Administration, Office of Research and Development Washington, DC, 2006.